INSTITUTE OF PHYSICS PUBLISHING JOURNAL OF PHYSICS A: MATHEMATICAL AND GENERAL

J. Phys. A: Math. Gen. **39** (2006) 4485–4491 doi:10.1088/0305-4470/39/17/S27

Two-dimensional Yukawa liquids: structure and collective excitations

P Hartmann[1], G J Kalman[2] and Z Donkó[1]

[1] Research Institute for Solid State Physics and Optics of the Hungarian Academy of Sciences, H-1525 Budapest, PO Box 49, Hungary
[2] Department of Physics, Boston College, Chestnut Hill, MA 02467, USA

E-mail: hartmann@sunserv.kfki.hu

Received 19 September 2005, in final form 22 December 2005
Published 7 April 2006
Online at stacks.iop.org/JPhysA/39/4485

Abstract

The paper reports molecular dynamics (MD) simulations on two-dimensional, strongly-coulped Yukawa liquids. An effective coupling coefficient Γ^* for the liquid phase is identified; thermodynamic properties such as internal energy, pressure and compressibility, as well as longitudinal and transverse mode dispersions are analysed.

PACS numbers: 52.27.Gr, 05.20.−y, 73.21.−b

1. Introduction

The Yukawa (screened Coulomb) potential $\phi(r) = \frac{Q^2}{r}\exp(-\kappa r)$ is a widely used approximation to describe the interaction of particles in a variety of physical systems, e.g. dusty plasmas [1] and charged colloids [2]. Many-particle systems with Yukawa interaction can be fully characterized by two dimensionless parameters: (i) the *coupling parameter* $\Gamma = \beta Q^2/a$ (where Q is the charge of the particles, a is the Wigner–Seitz radius and $\beta = 1/k_{\mathrm{B}}T$ is the inverse temperature), and (ii) the *screening parameter* κ. Besides three-dimensional (3D) systems, two-dimensional (2D) configurations also appear in a variety of physical systems. As examples, layers of dust particles formed in low pressure gas discharges may be mentioned.

The purpose of this work is to give an overview about the static and dynamic properties of strongly coupled 2D Yukawa liquids near thermal equilibrium conditions. The properties of the system are analysed with the aid of molecular dynamics simulations based on the PPPM (particle–particle particle–mesh) algorithm [4]; for more details of the implementation see [5]. The primary output data of our simulations are the pair correlation functions (PCF-s) $g(r)$, which are used as input data for the calculation of the correlational energy, pressure and compressibility and the static structure function $S(k)$. In addition, we generate the bond-angular order parameter G_Θ (see (4)). The solid-to-liquid transition is studied through monitoring the temperature dependence of the latter.

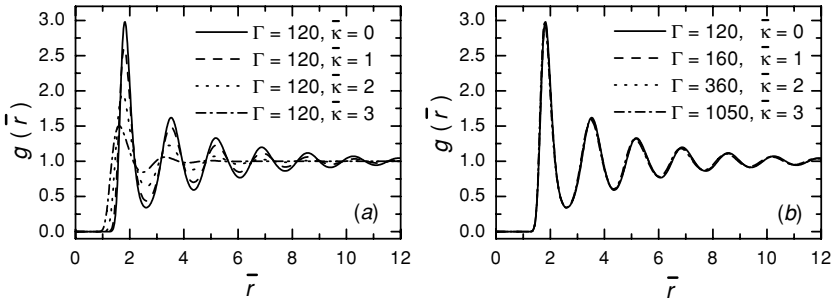

Figure 1. Pair correlation functions of the 2D Yukawa liquid for (*a*) $\Gamma = 120$ and different values of $\bar{\kappa}$, and (*b*) for $(\Gamma, \bar{\kappa})$ pairs corresponding to a constant $\Gamma^* = 120$.

Our simulations also provide information about the spectra of the longitudinal and transverse current fluctuations. These spectra are obtained through the Fourier transform of microscopic quantities [7]

$$L(k,\omega) = \left|\mathcal{F}\left\{k\sum_j v_{jx}\exp(\mathrm{i}kx_j)\right\}\right|^2, \qquad T(k,\omega) = \left|\mathcal{F}\left\{k\sum_j v_{jy}\exp(\mathrm{i}kx_j)\right\}\right|^2, \tag{1}$$

where the index j runs over all particles.

The spectra defined by (1) serve as the basis for the analysis of the collective excitations of the system. We have reported detailed calculations on this topic in [6].

In the following, the simulation results are given with the length scale normalized to the 2D Wigner–Seitz radius $a = (\pi n)^{-1/2}$ (where n is the areal density), i.e. $\bar{r} = r/a$, $\bar{\kappa} = \kappa a$ and $\bar{k} = ka$ for the wavenumber.

2. Static properties

The issue of scaling, i.e. whether only some combination of the Γ and $\bar{\kappa}$ parameters rather than both of these parameters independently, or, alternatively, the ratio of the temperature to the melting temperature govern the behaviour of Yukawa systems has been addressed by several studies: the universal scaling of structural properties and transport parameters has continued to receive attention for many years [8]. Here we establish a novel criterion for Γ^* effective coupling parameter that relies on associating a constant amplitude of the first peak of the PCF $[g(r)]$ with a constant Γ^* value.

The pair correlation functions of the 2D Yukawa liquid are displayed in figure 1(*a*) for $\Gamma = 120$ and for a series of $\bar{\kappa}$ values. It can be seen that the range of the rather pronounced order, characteristic for $\bar{\kappa} = 0$ rapidly diminishes with increasing $\bar{\kappa}$. The amplitude of the first peak of the PCF can, however, be re-established if Γ is also increased together with $\bar{\kappa}$. In fact, as figure 1(*b*) shows, within the range of $\bar{r}$ displayed not only the amplitude of the first peak, but the $g(\bar{r})$ functions in their entireties are nearly the same for fixed Γ^* values. (This scaling, however, does not apply to the tail of $g(r)$, cf [5].)

Figure 2(*a*) shows the contours on the Γ–$\bar{\kappa}$ plane which belong to constant effective coupling values $\Gamma^* = 120$, 40 and 10. It can be seen that these lines have approximately the same shape; thus they can be scaled to a single universal line, as shown in figure 2(*b*), which

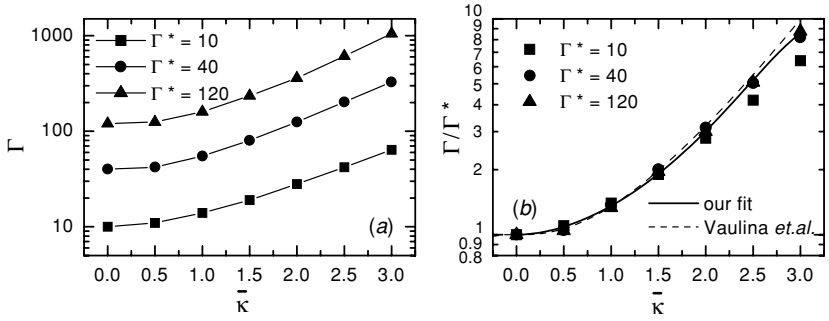

Figure 2. (*a*) Constant effective coupling (Γ^*) lines on the Γ–$\bar{\kappa}$ plane. (*b*) Dependence of the ratio Γ/Γ^* on $\bar{\kappa}$. The symbols are data taken from (a), while the solid line is a fit according to (2) and (3). The dashed line is the universality relation of Vaulina *et al* [9].

displays the dependence of the ratio Γ/Γ^* on $\bar{\kappa}$ for the chosen values of Γ^*. Our aim now is to find an $f(\bar{\kappa})$ function that allows us to partition $\Gamma^*(\Gamma, \bar{\kappa})$ as

$$\Gamma^* = \Gamma f(\bar{\kappa}). \tag{2}$$

At high values of Γ^* the ratio Γ/Γ^* depends only on $\bar{\kappa}$, the partitioning given in (2) is indeed possible, and $f(\bar{\kappa})$ can be fitted with the aid of the formula

$$\begin{aligned} &f(\bar{\kappa}) = 1 + f_2\bar{\kappa}^2 + f_3\bar{\kappa}^3 + f_4\bar{\kappa}^4, \qquad \text{with} \\ &f_2 = -0.388, \qquad f_3 = 0.138, \qquad f_4 = -0.0138. \end{aligned} \tag{3}$$

The universality scaling relation introduced by Vaulina and coworkers [8, 9] for 3D dusty plasmas based on transport phenomena (where $f(\bar{\kappa}) = (1 + \sqrt{\pi}\bar{\kappa} + \pi/2\bar{\kappa}^2)\exp(-\sqrt{\pi}\bar{\kappa})$) shows a remarkably good agreement with our present results for 2D Yukawa systems based on the PCF first peak amplitude.

The bond-angular order parameter G_Θ for a system with hexagonal symmetry [10, 11] has the form

$$G_\Theta = \frac{1}{N}\left|\sum_{l=1}^{N}\frac{1}{6}\sum_{m=1}^{6}\exp(\mathrm{i}6\Theta_{l,m})\right|^2, \tag{4}$$

where the subscript l runs over all particles of the system, and m runs over the neighbours of the lth particle, respectively; $\Theta_{l,m}$ is the angle between a fixed (e.g. x) direction and the vector connecting the lth and mth particles. The solid-to-liquid transition can be identified by a drop of the bond-angular order parameter below the empirical value $G_\Theta \cong 0.45$ [11–13].

The melting 'experiment' of the 2D Yukawa layer is illustrated in figure 3(*a*). After proper cooling of the system below freezing, the temperature is slowly increased and the bond-angular order parameter G_Θ is calculated according to (4) in each time step. With the increasing temperature, first we observe a slow decay of G_Θ (from an initial value close to 1.0, indicating nearly perfect hexagonal order); when the temperature reaches a critical value, G_Θ is seen to suddenly drop to $\approx$0, indicating an abrupt loss of the long-range orientational order in the system. We identify this event as the solid-to-liquid transition, taking place at $\Gamma = \Gamma_\mathrm{m}$. The temperature control of the system is realized by the Nosé–Hoover algorithm (see e.g. [14]).

The Γ_m–$\bar{\kappa}$ phase boundary, obtained from simulations illustrated above, is plotted in figure 3(*b*). At $\bar{\kappa} = 0$ the simulations closely reproduce the value $\Gamma_\mathrm{m}^\mathrm{Coulomb} \cong 137$ for the 2D one-component plasma (OCP) [15]. The present method does not make it possible to identify

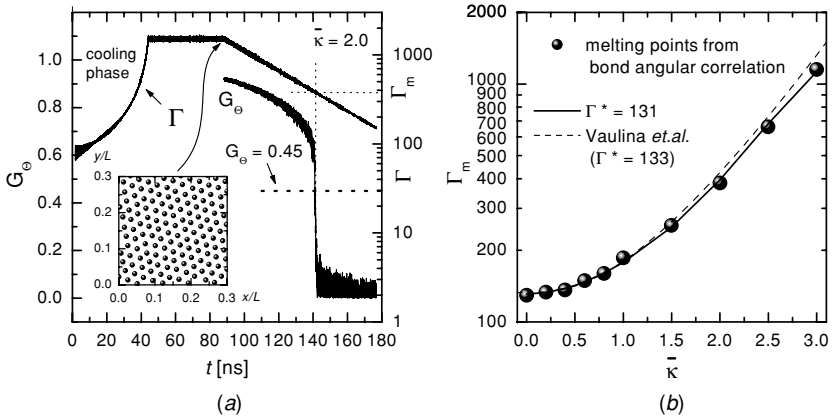

Figure 3. (*a*) Illustration of the 'melting experiment': time dependence of the bond-angular order parameter G_Θ and system temperature T, obtained at $\bar{\kappa} = 2$. The sudden decay of G_Θ below the 0.45 value [11]—marking the solid → liquid transition—occurs at $\Gamma_m = 384$. The inset shows a snapshot of particle positions recorded right before the temperature starts to increase. (*b*) Γ_m as a function of $\bar{\kappa}$ as obtained from the 'melting experiments' (symbols) and the $\Gamma^* = 131$ line. The dashed line is the scaling relation of Vaulina *et al* [9] with $\Gamma^* = 133$.

the theoretically predicted [10, 16] intermediate (so-called 'hexatic') phase between the solid and liquid states of the plasma.

The figure also shows the Γ values calculated from (3), assuming $\Gamma^* = 131$. We find an excellent agreement with the simulation data, which shows that the first peak amplitude of the PCF is nearly constant along the melting line of 2D Yukawa systems, regardless of the value of $\bar{\kappa}$, as already pointed out before.

The energy E (per particle), the pressure P and the inverse compressibility L of the system consist of the thermal part, the positive Hartree part and the negative correlational part. In the following, we focus our attention on the correlational component of these thermodynamic properties, which can be obtained from the PCF using the function $h(r) = g(r) - 1$.

$$\begin{aligned} \beta E_c &= \beta \frac{n}{2} \int h(r)\phi(r)\,\mathrm{d}\mathbf{r} = \Gamma \int_0^\infty h(\bar{r})\,\mathrm{e}^{-\bar{\kappa}\bar{r}}\mathrm{d}\bar{r} \\ \beta P_c &= -\beta \frac{n^2}{4} \int r \frac{\partial\phi(r)}{\partial r} h(r)\,\mathrm{d}\mathbf{r} = \frac{n\Gamma}{2} \int_0^\infty \bar{r}\left[\bar{\kappa} + \frac{1}{\bar{r}}\right]\mathrm{e}^{-\bar{\kappa}\bar{r}} h(\bar{r})\,\mathrm{d}\bar{r}. \end{aligned} \tag{5}$$

The data shown in figure 4(*a*) for E_c can be approximated as

$$\begin{aligned} &\beta E_c = \Gamma[b(\bar{\kappa}) + c(\bar{\kappa})\Gamma^{*-2/3}], \qquad \text{with} \\ &b(\bar{\kappa}) = b_0 + b_1\bar{\kappa} + b_2\bar{\kappa}^2 + b_3\bar{\kappa}^3 + b_4\bar{\kappa}^4 \qquad \text{and} \\ &c(\bar{\kappa}) = c_0 + c_1\bar{\kappa} + c_2\bar{\kappa}^2 + c_3\bar{\kappa}^3 + c_4\bar{\kappa}^4. \end{aligned} \tag{6}$$

where $b_0 = -1.103, b_1 = 0.505, b_2 = -0.107, b_3 = 0.006\,86, b_4 = 0.0005$; and $c_0 = 0.384, c_1 = -0.036, c_2 = -0.052, c_3 = 0.0176, c_4 = 0.001\,65$. Our data are in an excellent agreement with the energy values recently calculated [3] and at $\kappa = 0$ with the energy values given for the 2D OCP [3, 17].

The correlational part of the pressure is plotted in figure 4(*b*). Similarly to the energy, the data are in an excellent agreement with those qouted in [3]. In the $5 \leqslant \Gamma \leqslant 120$ and $0.5 \leqslant \bar{\kappa} \leqslant 3$ intervals the correlational part of the pressure (P_c) can be fitted using the form

$$\beta P_c = n\Gamma(b_0' + b_1'\bar{\kappa}), \qquad \text{where} \qquad b_0' = -0.5638 \qquad \text{and} \qquad b_1' = 0.09367. \tag{7}$$

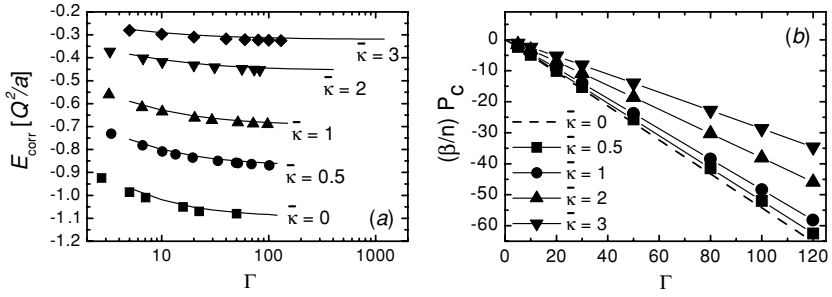

Figure 4. (*a*) Correlation energy per particle of the 2D Yukawa liquid as a function of Γ, for selected values of $\bar{\kappa}$. Lines: present results, symbols: [3]. (*b*) Correlational part of the pressure ($\beta P_c/n$) as a function of Γ for $\bar{\kappa} = 0.5$, 1, 2 and 3. The dashed line shows the behaviour of the pure Coulomb OCP [3, 17].

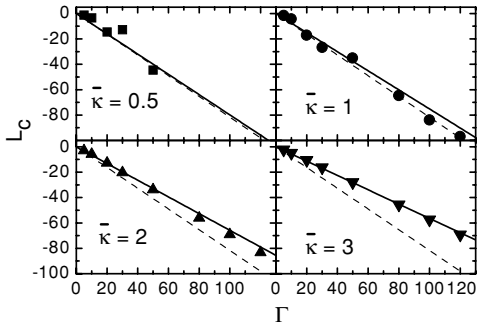

Figure 5. Correlational inverse compressibility L_C as a function of Γ for different $\bar{\kappa}$ values. Lines show data based on the equation-of-state calculation [through (8)], symbols show points calculated using the structure function $S(k)$ [through (9)]. The dashed lines show the behaviour of pure Coulombic OCP.

The correlational part of the inverse compressibility L_c is obtained from the pressure through the relation $L_c = \beta(\partial P_c/\partial n)$. Based on the fitting formula (7) L_c becomes

$$L_c = \beta\frac{\partial P_c}{\partial n} = \left(\frac{3}{2}b_0' + b_1'\bar{\kappa}\right)\Gamma = (-0.8458 + 0.093\,67\bar{\kappa})\Gamma. \tag{8}$$

If, on the other hand, the static structure function $S(k)$ is known, L_c can be determined directly from $S_0 = S(k = 0)$ through the compressibility sum rule [5] as

$$L_c = \frac{1}{S_0} - \frac{2\Gamma}{\bar{\kappa}} - 1. \tag{9}$$

The outcomes of the two independent calculations are compared in figure 5. A strong coincidence of the two sets of results, especially for larger $\bar{\kappa}$ values, verifies the consistency of the computational procedure.

3. Dynamic properties

The spectra of the longitudinal and transverse current fluctuations, $L(\bar{k}, \omega)$ and $T(\bar{k}, \omega)$ respectively, are displayed in the form of colour maps in figure 6, for the $\Gamma = 360$, $\bar{\kappa} = 2$ case. The spectra of the longitudinal current fluctuations show that at small $\bar{k}$ the mode frequency

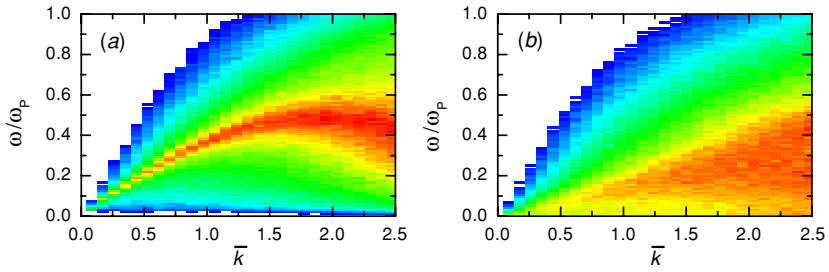

Figure 6. (*a*) Longitudinal $L(\bar{k}, \omega)$ and (*b*) transverse $T(\bar{k}, \omega)$ current fluctuations obtained at $\Gamma = 360$, $\bar{\kappa} = 2$. (The shading of the amplitude is logarithmic, it only intends to illustrate qualitative features.)

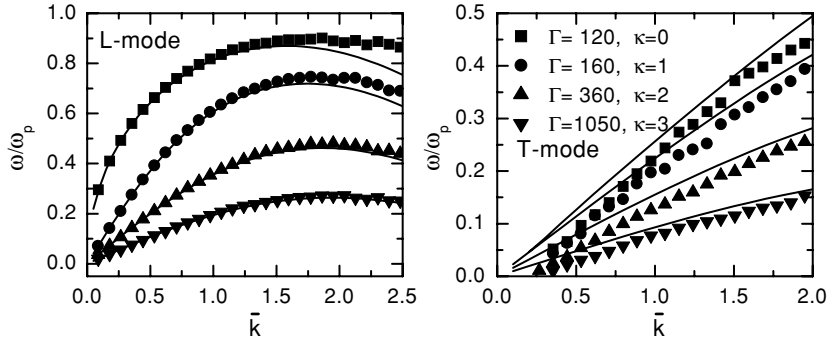

Figure 7. Dispersion curves for the longitudinal (L) and transverse (T) modes at $\Gamma^* = 120$ and $\bar{\kappa} = 0, 1, 2, 3$. Lines: QLCA calculations [6].

increases linearly with $\bar{k}$, then within a relatively wide range of $\bar{k}$ the mode frequency is near to $\omega/\omega_p \approx 0.45$, where $\omega_p = \sqrt{2\pi Q^2 n/ma}$ is the 2D nominal plasma frequency. The $T(\bar{k}, \omega)$ spectra (see figure 6(*b*)) are, as compared to the $L(\bar{k}, \omega)$ spectra, broader for any $\bar{k}$ value: the fluctuations in the transverse currents are distributed over a rather broad frequency domain.

The dispersion curves for both modes of the 2D Yukawa liquid are displayed in figure 7, together with $\bar{\kappa} = 0$ curves which represent a 2D Coulomb system [17]. With increasing $\bar{\kappa}$ the mode frequencies rapidly diminish. In the $k \to 0$ limit both modes exhibit an acoustic behaviour. All the described behaviour is in an excellent agreement with theoretical predictions based on the quasilocalized charge approximation [5].

Acknowledgments

This work has been supported by the Hungarian Fund for Scientific Research Grant OTKA-T-48389, OTKA-PD-049991, MTA-OTKA-90/46140, NSF Grant PHYS-0206695, DOE Grant No. DE-FG02-03ER5471 and NSF Grant No. PHYS-0514619.

References

[1] Melzer A, Schweigert V A, Schweigert I V, Homann A, Peters S and Piel A 1996 *Phys. Rev.* E **54** R46
Pieper J B, Goree J and Quinn R A 1996 *J. Vac. Sci. Technol.* **14** 519
Sternovsky Z, Lampe M and Robertson S 2004 *IEEE Trans. Plasma Sci.* **32** 632

Krauss C E, Horányi M and Robertson S 2003 *New J. Phys.* **5** 70
[2] Löwen H 2003 *J. Phys. A: Math. Gen.* **36** 5827
Hynninen A P and Dijkstra M 2003 *J. Phys.: Condens. Matter* **15** S3557
Auer S and Frenkel D 2002 *J. Phys.: Condens. Matter* **14** 7667
[3] Totsuji H, Liman M S, Totsuji C and Tsuruta K 2004 *Phys. Rev.* E **70** 016405
[4] Hockney R W and Eastwood J W 1981 *Computer Simulation Using Particles* (New York: McGraw-Hill)
[5] Hartmann P, Kalman G J, Donkó Z and Kutasi K 2005 *Phys. Rev.* E **72** 026409
[6] Kalman G J, Hartmann P, Donkó Z and Rosenberg M 2004 *Phys. Rev. Lett.* **92** 065001
[7] Hansen J-P, McDonald I R and Pollock E L *Phys. Rev.* A **11** 1025
Hamaguchi S 1999 *Plasmas Ions* **2** 57
[8] Rosenfeld Y 2001 *J. Phys.: Condens. Matter* **13** L39
Ohta H and Hamaguchi S 2000 *Phys. Plasmas* **7** 4506
Saigo T and Hamaguchi S 2002 *Phys. Plasmas* **9** 1210
Vaulina O, Khrapak S and Morfill G 2002 *Phys. Rev.* E **66** 016404
Vaulina O and Vladimirov S V 2002 *Phys. Plasmas* **9** 835
Fortov V E *et al* 2003 *Phys. Rev. Lett.* **90** 245005
Faussurier G and Murillo M S 2003 *Phys. Rev.* E **67** 046404
Faussurier G 2004 *Phys. Rev.* E **69** 066402
[9] Vaulina O S and Khrapak S A 2000 *JETP* **90** 287
[10] Halperin B I and Nelson D R 1978 *Phys. Rev. Lett.* **41** 121
[11] Schweigert I V, Schweigert V A and Peeters F M 1999 *Phys. Rev. Lett.* **82** 5293
[12] Löwen H 1992 *J. Phys. C: Solid State Phys.* **4** 10105
[13] Morfill G E, Thomas H M, Konopka U and Zuzic M 1999 *Phys. Plasmas* **6** 1769
[14] Frenkel D and Smit B 2001 *Understanding Molecular Dynamics Simulations* (New York: Academic)
[15] Grimes C C and Adams G 1979 *Phys. Rev. Lett.* **42** 795
[16] Chui S T 1982 *Phys. Rev. Lett.* **48** 933
Aeppli G and Bruinsma R 1984 *Phys. Rev. Lett.* **53** 2133
Strandburg K J 1988 *Rev. Mod. Phys.* **60** 161–207
Ryzhov V N and Tareyeva E E 1995 *Phys. Rev.* B **51** 8789
[17] Golden K I, Kalman G J and Wyns P 1992 *Phys. Rev.* A **46** 3463